Urol Res (2006) 34: 200–210
DOI 10.1007/s00240-006-0043-7

ORIGINAL PAPER

**Susan Ruth Marengo · Daniel H.-C. Chen
Andrew P. Evan · Andre J. Sommer · Nicholas T. Stowe
Donald G. Ferguson · Martin I. Resnick
Gregory T. MacLennan**

Continuous infusion of oxalate by minipumps induces calcium oxalate nephrocalcinosis

Received: 15 November 2005 / Accepted: 17 January 2006 / Published online: 15 February 2006

Abstract It is hypothesized that oxalate plays an active role in calcium oxalate (CaOx) nephrocalcinosis and oxalate driven nephrolithiasis by interacting with the kidney. We developed an adjustable, nonprecursor, continuous infusion model of hyperoxaluria and CaOx nephrocalcinosis to investigate this hypothesis. Minipumps containing PBS or KOx (60–360 μmol/day; $n = 5$–7/dose) were implanted subcutaneously in male Sprague–Dawley rats on D0 and D6. Rats were killed on D13. Oxalate excretion and CaOx crystalluria were monitored by 20 + 4 h urine collections. Localization and content of intrarenal crystals were determined on frozen sections using polarization and μFTIR. Oxalate excretion was significantly elevated in all KOx rats ($P \leq 0.005$). CaOx crystalluria was most persistent in the 240–360 μmol/day KOx rats, but even 60 μmol/day KOx rats showed sporadic crystalluria. One hundred percent of KOx rats had CaOx nephrocalcinosis as confirmed by μFTIR. Most crystals were localized to the lumens of the corticomedullary collecting ducts. A few crystals are localized just under the papillar urothelium. The minipump model is the first model of hyperoxaluria to provide continuous infusion of oxalate. It permits control of the levels of hyperoxaluria, crystalluria and CaOx nephrocalcinosis. The level of sustained hyperoxaluria and CaOx nephrocalcinosis induced by treatment with 360 μmol/day KOx for 13D models the conditions frequently observed in jejunoileal bypass patients. Adjustments in the length of treatment and level of hyperoxaluria may allow this model to also be used to study the oxalate driven CaOx-nephrolithiasis common in patients with hyperoxaluria due to other causes.

Keywords Nephrocalcinosis · Nephrolithiasis · Calcium · Oxalate · Oxalosis · Rat

S. R. Marengo (✉) · D. H.-C. Chen · M. I. Resnick
Department of Urology, School of Medicine,
Case Western Reserve University, 10900 Euclid Ave,
Cleveland, OH 44106-4931, USA
E-mail: srm10@case.edu
Tel.: +1-216-3688732
Fax: +1-216-3680213

A. P. Evan
Department of Anatomy and Cell Biology, Indiana University School of Medicine, Indianapolis, IN, USA

A. J. Sommer
Department of Chemistry and Biochemistry, Miami University, Oxford, OH, USA

N. T. Stowe
Department of Surgery, School of Medicine,
Case Western Reserve University, Cleveland, OH, USA

D. G. Ferguson
Department of Anatomy, School of Medicine,
Case Western Reserve University, Cleveland, OH, USA

G. T. MacLennan
Institute of Pathology, School of Medicine,
Case Western Reserve University, Cleveland, OH, USA

Introduction

The role that oxalate plays in calcium oxalate (CaOx) nephrocalcinosis (deposition of crystals within the kidney proper) and oxalate driven nephrolithiasis (Ox-nephrolithiasis, formation of a stone or gravel within the extrarenal spaces) is not well understood. There are several conditions which result in sustained hyperoxaluria. All patients with primary hyperoxaluria type I develop CaOx-nephrocalcinosis and Ox-nephrolithiasis [1]. In contrast, only a proportion of those patients with primary hyperoxaluria type II [1], inflammatory bowel disease [2], jejunoileal bypass surgery [3, 4], cystic fibrosis [5], or idiopathic hyperoxaluria [6, 7] develop Ox-nephrolithiasis, or less frequently, CaOx-nephrocalcinosis. Oxalate excretion is highly variable in CaOx stone formers, so even though 39% of idiopathic stone formers have oxalate excretions at the high end of normal (40–45 mg/24 h [8]), many studies report no significant difference in oxalate excretion between stone

formers and normal individuals [6, 7]. Current thinking is that many idiopathic CaOx stone formers experience only transient elevations in urinary oxalate due to variations in such factors as diet or hydration and that their stone disease is related to hypercalciuria with resultant Randall's plaque formation [9]. In their now classic studies of rats treated with oxamide or ethylene glycol, Vermeulen and Lyon [10] hypothesized that CaOx stone disease was the result of a high "triggering" dose of oxalate followed by an extended period of exposure to lower "maintenance" levels of oxalate. More recent data supporting this hypothesis is provided by Khan et al. [11, 12] who demonstrated that a continuous 2× elevation in urinary oxalate plus a bolus injection of oxalate can induce CaOx nephrocalcinosis. Furthermore, it has recently been shown that the consumption of a dose of oxalate equivalent to that found in a single serving of spinach can transiently elevate urinary oxalate excretion into the range seen in patients with primary hyperoxaluria [13].

It has been calculated that fluid only takes about 3 min to traverse the nephron, although it takes about 41 min for a CaOx crystal to grow to clinically relevant size [14]. This means that crystal retention within the kidney, either by attachment to the renal epithelium or by formation of aggregates, is essential if nephrocalcinosis is to develop. Many researchers now hypothesize that oxalate promotes crystal formation and retention through its effects on renal epithelial cell physiology [15–18]. Among its many effects, oxalate can promote cell death, cell proliferation, and increased binding of CaOx to renal epithelial cell membranes [19, 20]. Cells that are proliferating or physically damaged bind more CaOx than those comprising a mature monolayer [21, 22]. The presence of cellular debris can also promote nucleation and aggregation [23]. We hypothesize that there is a broad range of sensitivity to oxalate which could, in part, explain the apparent disconnect between oxalate excretion and the incidence of CaOx-nephrocalcinosis.

The study of how oxalate interacts with the kidney to promote crystal formation, retention and deposition has been hampered by the lack of an appropriate animal model. An in vivo model would allow investigations to be performed on a fully differentiated epithelium with all endocrine and paracrine regulatory pathways and anatomical features intact. Importantly, multiple segments or tissue compartments could be studied. An in vivo model would also facilitate investigation of oxalate's effects on other organs or on how oxalate is partitioned for excretion. We have refurbished the minipump model of hyperoxaluria [11, 24], which uses osmotic minipumps implanted subcutaneously to deliver oxalate continuously and steadily for periods of up to 14 days. In addition to studying the interactions between oxalate and the kidney which promote the development of nephrocalcinosis, the minipump model could serve as an important bridge between in vitro studies and animal models of oxalate driven nephrolithiasis that are tailored to form nephroliths in a time frame and at oxalate dosages seen in patients with secondary or idiopathic hyperoxaluria. In the refurbished minipump model we can regulate the degree of hyperoxaluria, frequency of CaOx crystalluria, and the extent of CaOx-nephrocalcinosis.

Materials and methods

Implantation of osmotic minipumps

Male Sprague–Dawley rats (200–250 g) were obtained from Harlan (Indianapolis, IN) and maintained under standard conditions at the Case Animal Resource Center. Rats were given 5 days to acclimatize prior to use. Food and water were available ad libidum.

Alzet® osmotic minipumps (Durect, Cupertino, CA) with 2 ml reservoirs and a 1 week life span were filled and implanted according to the manufacturer's instructions. Minipumps were handled at a surgical plane of sterility at all times. Minipumps were filled with 2 ml of phosphate buffered saline vehicle (PBS) or the appropriate dosage of potassium oxalate (KOx), $n = 5$–7 rats/dose: 0.25 M (60 μmol/day); 0.5 M (120 μmol/day); 1 M (240 μmol/day); 1.25 M (300 μmol/day); or 1.5 M (360 μmol/day). KOx was filtered (0.2 μm) prior to each use to remove any precipitated crystals. Minipumps were primed for 24 h by soaking in PBS at 25°C. To confirm that minipumps were in the plateau phase of delivery during the entire treatment period, three minipumps were filled with 360 μmol/day KOx and ^{14}C-oxalic acid (^{14}C-Ox; 7.1 mCi/mmol, Sigma, St. Louis, MO). Pumps were primed at 25°C for 24 h and then incubated in PBS at 37°C in 30 ml PBS; PBS was replaced daily and the ^{14}C-Ox release was determined by scintillation counting.

Each rat was anesthetized using a cocktail of 42.8 mg/ml ketamine, 8.6 mg/ml xylazine and 1.4 mg/ml acepromazine (i.m., 0.1–0.2 ml/100 g). The surgical field was infiltrated with 1 ml of a 0.025% solution of Bupivacaine to provide 8–10 h of analgesia. A 1.5 cm incision was made over the shoulder and a pair of hemostats was used to create a subcutaneous pocket running posteriorly. A minipump was inserted portal first and the wound was closed with 3–4 clips. After 6 days (implantation = D0) the spent minipump was removed, the cavity flushed with 20 ml of warm PBS, and the wound closed. The replacement pump was inserted in the contralateral shoulder. Rats were monitored postoperatively in accordance with ARC guidelines. After 13 days, rats were sacrificed by means of an overdose of anesthesia cocktail.

Processing of urine, plasma and tissue

Twenty-four hour urine collections were performed beginning 24 h prior to implantation (D-1-0) and on

days 2–3 (D3), 5–6 (D6), 9–10 (D10) and 12–13 (D13) following implantation. During the collection period rats were placed in metabolic cages (UniFab, Kalamazoo, MI) and urine was collected without adding preservatives at 4°C and then stored at −20°C. Urine samples (4 h) were taken at room temperature, centrifuged, washed in PBS and inspected for crystals using light microscopy at 100×. On D13 blood samples were drawn from the tail artery of each anesthetized rat using heparinized syringes. Blood pH was determined immediately on a blood-gas analyzer (Radiometer, Copenhagen). Additional blood was collected by cardiac puncture using heparinized syringes and the plasma was stored at −80°C. Urine samples were collected from the bladders immediately following exsanguination and the pH (pH paper with 0.3 unit gradations, Whatman, Florham Park, NJ) and specific gravity (dipstick, Chemstrip, Roche, Indianapolis, IN) were determined. Urine oxalate concentrations were determined by the oxalate-oxidase colorimetric assay (Trinity Biotech, Brae, Ireland). Assays for plasma and urine creatinine and ion concentrations were performed by the Core Laboratory of the University Hospitals of Cleveland. Levels of C-reactive protein (CRP) were determined in plasma by ELISA (BD Biosciences, Franklin Lakes, NJ). Transverse cross sections of the kidney containing the cortex, medulla and papilla were fixed in 4% paraformaldehyde, embedded in paraffin and stained with H&E by the Rainbow Babies and Children's Pathology Core. Calcious deposits were detected by the Yasue silver substitution method [25]. Other transverse cross sections, unfixed, were frozen in an isopentane-lq N_2 cooled bath, stored in lq N_2 vapor and cryosectioned.

Fourier transform infrared microspectroscopy (μ-FTIR)

Kidneys were snap frozen and stored at −80°C. At sectioning kidneys were embedded in OCT compound (Miles Laboratories, Elkhart, IN) and serial cryosections cut in the midtransverse plane, generating perfect cross sections showing outer cortex to papillary tip. Even sections were mounted on low-E glass slides for infrared analysis of mineral composition and fixed in acetone for 15–20 s. Odd sections were fixed in acetone, stained with 1% Toluidine Blue, dehydrated and cover slipped. The composition of crystal deposits in situ was determined by attenuated total internal reflection (ART) μ-FTIR. [9, 26, 27]. All sites of mineral deposition in a given cross section were analyzed. Infrared spectra were collected with a Perkins-Elmer Auto Image infrared microscope interfaced to a Perkins-Elmer Spectrum 2000 Fourier transform spectrometer in the Molecular Micro spectroscopy Laboratory of Dr. J Andre Sommer, Department of Chemistry and Biochemistry, Miami University, Oxford, Ohio. This new system employs a 250×250 μm, liquid nitrogen cooled, mercury cadmium telluride detector (Hectic). Samples were analyzed using a 50×50 μm aperture. Each spectrum represents the average of 64 individual scans with 4 cm^{-1} spectral resolution. Infrared spectra were also collected for standards (calcium oxalate, calcium carbonate and hydroxyapatite) and regions of tissue and embedding medium were scanned for comparison. The relative infrared sensitivities were determined from the absorbance of a sample of known thickness.

In an effort to assess the sensitivity of μ-FTIR for the study of the crystal deposits, the relative infrared sensitivities were determined from the absorbance of a given sample with a known thickness. Sensitivities for the oxalate band (1,632 band) and the hydroxyapatite band (1,029 band) were 0.275 and 0.136, respectively. Based on these values μ-FTIR is approximately two times more sensitive for oxalate than it is for hydroxyapatite. However, due to the presence of an interfering amide I absorption from the tissue located at 1,640 cm^{-1}, oxalate was identified by using the 769 cm^{-1} band. This band has an infrared sensitivity of 0.090, thereby favoring the detection of hydroxyl apatite by a factor of 1.5x. We have recently published a paper detailing the issues one must consider when analyzing mineral deposits in tissues [27].

Inulin clearance

Rats were treated with 360 μmol/day KOx ($n = 5$) or PBS ($n = 5$) for 13 days according to the standard protocol. Inulin clearance was determined as previously described [28]. Briefly, each rat was anesthetized with Inactin (75 mg/kg) and placed on a heated platform. The trachea was intubated and the right external jugular vein cannulated for the infusion of a solution of 1% inulin in 0.9% saline at 0.6 ml/100 g body weight/h. The right carotid artery was cannulated for the measurement of blood pressure. A small midline incision was made to facilitate cannulation of the left ureter for the collection of urine. Following a 60 min equilibration period, inulin clearance was determined during three 20 min urine collection periods with a blood sample taken at the midpoint of each period. Inulin concentrations were determined colorimetrically by the resorcinol assay (A_{490}).

Statistical analysis

Analysis of variance (ANOVA) was used to determine whether the main treatment effects differed significantly between treatment groups (SPSS, Chicago, IL). If they differed significantly ($P \leq 0.05$), all six treatment groups were compared with each other using Tukey's test. Data are presented as mean ± standard error of the mean (SEM). Regression analysis was performed when appropriate using data from all six treatment groups (Graphpad Prism, San Diego, CA). There are several instances where our point can be made by comparing D13 data from only the 360 μmol/day KOx and PBS rats; in the interest of brevity we have done so.

Results

Minipump function

There was no difference in the mean residual volume of minipumps delivering PBS (339 ± 44 µl) and those delivering 360 µmol/day KOx (362 ± 21 µl; $P > 0.6$), indicating that the minipumps functioned equivalently regardless of the solution dispensed. The useable reservoir in these minipumps is 2,000 µl. With a release rate of 240 µl/day, the minipump contains 8.3 doses and has a theoretical pump life of 192 h. The first minipump was implanted on Tuesday (D0) and replaced on Monday (D6) for a duration of 144 h. The second minipump was removed on the second Monday (D13) for a duration of 168 h. Three minipumps were used to confirm that plateau levels of release were maintained during the entire treatment period; they were filled with 1.5 M KOx and ^{14}C-Ox. As expected, less ^{14}C-Ox was released during the priming phase than during the release phase (Fig. 1, $P \leq 0.001$). Thereafter minipumps maintained a steady release rate for 168 h at 37°C ($P > 0.1$). The amount of ^{14}C-Ox released between 168 and 192 h was reduced ~25% compared to earlier time points (24, 48, 96 h; $P \leq 0.01$). From these data we conclude that the minipumps are capable of delivering a constant dose of oxalate throughout the treatment period.

General response to treatment

Table 1 summarizes general parameters for D13 rats treated with PBS or 360 µmol/day KOx. The plasma concentrations of creatinine and the 24 h urinary excretion of creatinine did not differ between the two groups ($P > 0.3$). Both PBS and 360 µmol/day KOx rats had similar starting weights ($P > 0.6$), but 360 µmol/day KOx rats grew more slowly during treatment and had a lower final weight ($P \leq 0.002$). Food consumption per gram body weight did not differ between groups ($P > 0.1$).

As discussed in our preliminary report on this model [24], occasional foci of inflammation were observed in the kidneys of rats treated with 360 µmol/day KOx for 13D; a similar observation was made in the current study. These foci are frequently, but not always, associated with crystal deposits. To rule out that these foci either caused or resulted from a systemic inflammation, rat plasma was assayed by ELISA for CRP. CRP is a member of the pentraxin family and is an acute phase protein secreted by the liver [29–32]. It is an exquisitely sensitive marker for a variety of inflammatory responses and tissue damage including infections, localized necrosis, trauma and some cancers. Mean concentrations of CRP on D13 did not differ between PBS and 360 µmol/day KOx rats ($P > 0.$ 2, Table 1). No rat's concentration of CRP exceeded the upper limit of normal, 600 µg/ml [31, 32], and there was no correlation between average postimplantation oxalate excretion and D13 CRP ($r^2 = 0.077$, $P > 0.08$, $y = -0.0512x + 49.85$). Similarly, there was no correlation between oxalate dosage and CRP ($r^2 = 0.025$, $P > 0.3$, $y = 0.00085x + 0.4922$) or percentage weight gain and CRP ($r^2 = 0.032$, $P > 0.3$, $y = -0.01775x + 23.14$). From these data we concluded that oxalate does not induce systemic inflammation.

Consistent with our previous report, D13 urine output of 360 µmol/day KOx rats was 2-fold greater than that of PBS rats (Table 1; $P \leq 0.005$). Treatment did not affect the pH or specific gravity of voided urine or pH of blood (Table 1; $P > 0.1$). A separate experiment was performed to confirm that overall renal function was not

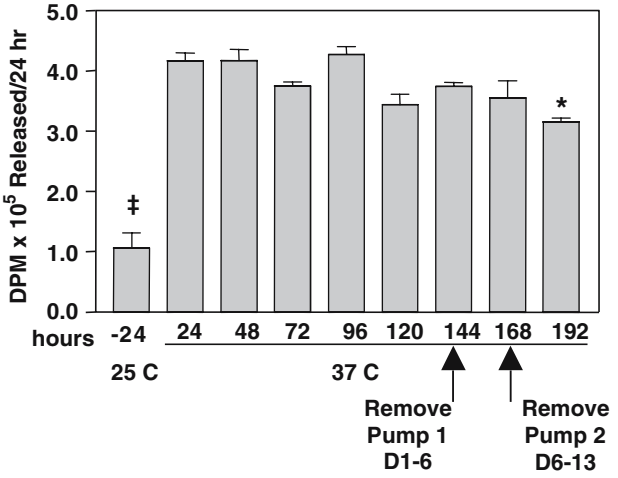

Fig. 1 Release of ^{14}C-oxalate from minipumps filled with 1.5 M KOx in PBS and then submerged in PBS at 25°C (−24 to 0 h = priming period) or 37°C (0–192 h = implantation). *Arrows* time when spent pumps are removed from the rats. *Different from 24, 48, and 96 h at $P \leq 0.025$. ‡Different from 37°C at $P \leq 0.001$. Mean ± SEM, $n = 3$

Table 1 Day 13 rat parameters for rats treated with PBS vehicle or 360 µmol KOx

	PBS ($n = 7$)	360 µmol/day KOx ($n = 7$)
Oxalate excretion (µmol/24 h)	6.9 ± 1.1	60.9 ± 5.2‡
Creatinine excretion (µmol/24 h)	91.7 ± 16.6	114 ± 13.0
Plasma creatinine (mg/dl)	0.46 ± 0.02	0.43 ± 0.04
Urine volume (ml/24 h)	11.1 ± 2.1	22.4 ± 2.4†
Starting body weight (g)	243 ± 11.4	249 ± 5.0
Final body weight (g)	302 ± 9.2	264 ± 3.8**
% Change in body weight	24 ± 2.6	6.3 ± 3.2**
Food/g body weight (mg/g)	81.3 ± 5.6	94.7 ± 5.5
C-reactive protein (µg/ml plasma)	305 ± 46.4	395 ± 41.1
Voided urine pH	6.7 ± 0.1	6.3 ± 0.2
Blood pH	7.43 ± 0.01	7.41 ± 0.02
Specific gravity	1.0129 ± 0.0015	1.0121 ± 0.0029
Residual pump volume (µl)	339 ± 44.1	363 ± 21.2

Values are mean ± SEM
**$P \leq 0.02$, †$P \leq 0.005$, ‡$P \leq 0.001$

impaired by treatment with 360 μmol/day KOx and that increased urine volume was not an artifact of water bottle leakage. Inulin clearance and direct renal output were determined in rats treated with PBS or 360 μmol/day KOx for 13D ($n = 5$ rats/dose). As can be seen in Table 2, there was no difference in kidney size or kidney size per gram of body weight between the two groups ($P > 0.05$). Inulin clearance did not differ between PBS and 360 μmol/day KOx rats ($P > 0.05$). Urine output per kidney and per gram kidney was significantly increased in 360 μmol/day KOx rats ($P \leq 0.02$), indicating a genuine increase in renal output.

Oxalate excretion and crystalluria

All six treatment groups had similar preimplantation oxalate excretions (overall mean 6.3 ± 0.5; $P > 0.2$). Oxalate excretion was similar in pre- and postimplantation PBS rats (6.2 ± 0.9 vs. 7.2 ± 0.5 μmol/day, $P > 0.5$). Figure 2 shows average and daily postimplantation oxalate excretions and the incidence of CaOx crystalluria. The average postimplantation oxalate excretions were higher in all groups of oxalate treated rats than in PBS treated rats ($P \leq 0.004$).

When the longitudinal analysis within treatment groups was performed, postimplantation oxalate excretions were always greater than preimplantation values ($P \leq 0.001$), with the exception of D6 in 120 μmol/day KOx rats ($P > 0.2$). There was an apparent decrease in oxalate excretion at D6 (144 h) in most of the treatment groups, despite our confirmation that minipumps are capable of delivering a constant dose of oxalate throughout the treatment period (Fig. 1). Exhaustive analysis between and within treatment groups failed to reveal any consistent differences between oxalate excretions at D6 and those at other postimplantation time points.

Based on crystal morphology and oil-immersion microscopy, the excreted crystals were CaOx-dihydrate. No samples showed CaOx crystalluria on D0. Five of the six rats treated with 60 μmol/day KOx showed crystalluria at least once during the postimplantation period. Crystalluria was sporadic in these rats and none showed crystalluria in more than two of the four postimplantation samples. Rats treated with 120 or 240 μmol/day KOx showed a biphasic pattern of CaOx crystalluria with the incidence being lowest at D6. One rat in each treatment group showed CaOx crystalluria in all postimplantation collections. CaOx crystals were detected in almost all of the postimplantation samples collected from rats treated with 300 or 360 μmol/day KOx.

Table 2 Day 13 inulin clearance by rats treated with PBS vehicle or 360 μmol KOx

	PBS ($n = 5$)	360 μmol/day KOx ($n = 5$)
Final body weight (g)	354 ± 13	313 ± 14
Kidney weight (g)	1.2 ± 0.02	1.2 ± 0.07
g Kidney/g body weight	0.35 ± 0.02	0.36 ± 0.02
Urine volume (μl/min)	3.7 ± 0.45	14.5 ± 3.2**
Urine volume μl/min/g kidney	2.9 ± 0.35	13.5 ± 3.6**
Inulin clearance ml/min	1.4 ± 0.15	1.2 ± 0.13
Inulin clearance ml/min/g kidney	1.4 ± 0.16	1.2 ± 0.13

Values are mean ± SEM
**$P \leq 0.02$

Plasma and urinary ions

The effects of treatment with 360 μmol/day KOx on plasma ions are shown in Table 3. Treatment with 360 μmol/day KOx did not affect the levels of any of the plasma ions tested ($P > 0.1$). The effects of treatment with PBS or 360 μmol/day KOx on D13 urinary ion excretions are shown in the first two columns of Table 4. Mean 24 h excretions of sodium ($P \leq 0.005$) and potassium were higher ($P \leq 0.05$) in 360 μmol/day KOx rats than in PBS rats, while those of calcium ($P \leq 0.001$), phosphate and magnesium were lower ($P \leq 0.05$; Table 4).

The excretion of many ions is tied directly or indirectly to water reabsorption. To determine whether the changes in ion excretion were more tightly correlated with oxalate excretion or urine volume, regression analysis using all six treatment groups was performed (last two columns of Table 4). As expected, urine volume and oxalate excretion were positively correlated ($r^2 = 0.26$; $P \leq 0.05$; $y = 0.2084x + 8.247$). The 24 h excretion of sodium, potassium, chloride and calcium was significantly correlated with oxalate excretion ($P \leq 0.02$). Urine volume was significantly correlated with sodium, potassium, chloride, urea ($P \leq 0.001$), calcium and magnesium excretion ($P \leq 0.05$). In many cases urine volume was more tightly correlated with ion excretion than was oxalate excretion. This suggests that changes in ion excretion may be a secondary effect due to oxalate-induced changes in renal physiology.

Deposition of intrarenal crystals

Intrarenal CaOx crystal deposition was determined on paraffin embedded tissues stained with H&E. Deposits were detected in 100% of the rats treated with 360 μmol/day KOx. Only 28% (2/7) of the 300 μmol/day KOx rats had intrarenal deposits of CaOx, and in both cases only a few deposits were observed in each section. One or two deposits were seen occasionally in sections from rats treated with lower dosages of oxalate. Most of the crystals were localized to the lumens of the collecting ducts near the corticomedullary junction (Fig. 3a). The identity of the deposits was confirmed in two ways. Firstly, pairs of serial sections were stained and observed by microscopy, one member of each pair using H&E and

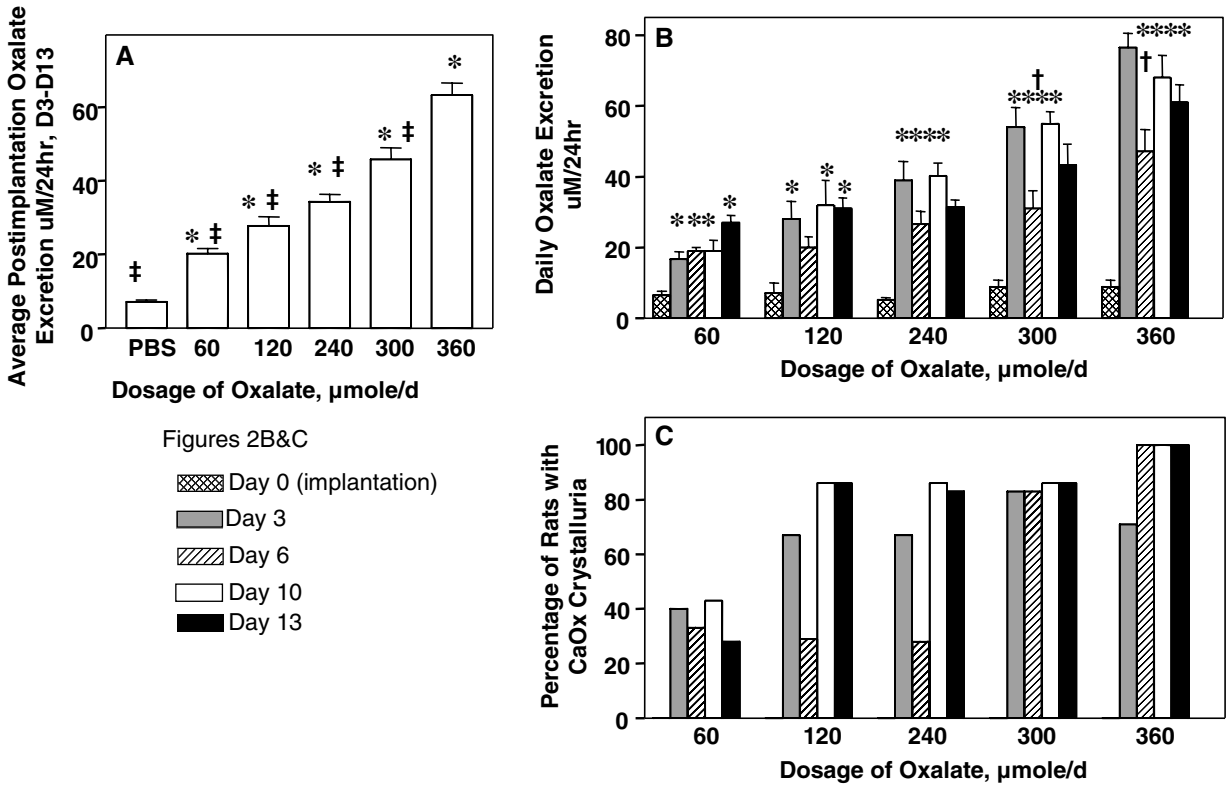

Fig. 2 Urinary excretion of oxalate and CaOx crystalluria by rats treated with PBS or 60–360 µmol/day KOx. **a** Overall mean postimplantation oxalate excretion. **b**, **c** Postimplantation oxalate excretion and CaOx crystalluria stratified by day and dose. *Different from PBS at $P \leq 0.004$. ‡Different from 360 µmol/day KOx at $P \leq 0.001$. †Different from all other days within the dosage at $P \leq 0.001$. Mean ± SEM, $n = 5$–7 rats per dose/time point

polarized light; the other using the Yasue silver substitution method (which stains calcious deposits reddish-black) and unpolarized light. Both protocols produced similar patterns of deposits (Fig. 3a, b), suggesting that the birefringent deposits did, indeed, contain calcium. Secondly, sections from rats treated with 360 µmol/day or 240 µmol/day KOx ($n = 3$/dose) were subjected to μ-FTIR spectroscopy. All crystalline deposits were composed of CaOx. Twenty percent of the samples contained a detectable, but not quantifiable, amount of calcium carbonate. No apatite was detected in any of the samples. A representative tracing is shown in Fig. 3c.

Table 3 Day 13 plasma ion concentrations in rats treated with PBS vehicle or 360 µmol KOx

	PBS ($n = 7$)	360 µmol/day Kox ($n = 7$)
Sodium (mM/l)	143 ± 1.2	140 ± 2.7
Potassium (mM/l)	4.9 ± 0.2	5.3 ± 0.1
Chloride (mM/l)	100 ± 1.1	98 ± 1.9
Calcium (mg/dl)	9.7 ± 0.2	9.8 ± 0.2
Blood urea nitrogen (mg/dl)	17.4 ± 0.6	17.7 ± 0.9
Phosphate (mg/dl)	10.4 ± 0.4	11.2 ± 0.8
Magnesium (mEq/l)	1.4 ± 0.04	1.6 ± 0.04

Values are mean ± SEM
$P > 0.1$ for all parameters

It surprised us that the percentage of rats having intrarenal CaOx deposits was so much lower in the 300 µmol/day KOx group than in the 360 µmol/day group, given that both dosages induced persistent crystalluria and that 300 µmol/day is only 17% less than 360 µmol/day. There were no differences between the 360 µmol/day and 300 µmol/day KOx groups in starting body weights, final weights, plasma levels of CRP, or average postimplantation urine volumes ($P \leq 0.2$; data not shown). Evan et al. [33] recently reported that tissue processing has a dramatic effect on the number of crystals observed in a given section. To determine whether processing artifact was responsible for the sudden decline in crystal deposition, cross sections were fixed by two protocols: (1) immersion fixation in paraformaldehye, embedding in paraffin and staining with H&E (Fig. 3d); and (2) snap freezing in an isopentane-lqN_2 cooled bath, cryosectioning, light fixation with glutaraldehyde, and staining with Toluidine blue (Fig. 3e). As in the previous report, frozen sections consistently showed more birefringent crystals under polarizing optics than did their paraffin embedded counterparts; however, this did not explain the dramatic decrease in crystal deposition at oxalate dosages of 300 µmol/day KOx and below.

Frozen sections revealed several important aspects of crystal localization that were not apparent in paraffin

Table 4 Day 13 urine ion excretion by rats treated with PBS vehicle or 60–360 μmol KOx

	PBS ($n=7$)	360 μmol/day KOx ($n=7$)	r^2 for 24 h oxalate PBS +60–360 μmol/day KOx ($n=41$)	r^2 for 24 h volume PBS + 60–360 μmol/day KOx ($n=41$)
Sodium (mM/24 h)	1.1 ± 0.09	1.4 ± 0.06†	0.31‡	0.56‡
Potassium (mM/24 h)	3.2 ± 0.3	4.2 ± 0.2*	0.18**	0.66‡
Chloride (mM/24 h)	2.1 ± 0.2	2.5 ± 0.1	0.17**	0.52‡
Calcium (mg/24 h)	1.9 ± 0.3	0.6 ± 0.1‡	0.14**	0.12*
Urea Nitrogen (mg/24 h)	309 ± 27	328 ± 15	0.05	0.54‡
Phosphate (mg/24 h)	14.3 ± 0.2.2	8.4 ± 0.8*	0.09	0.01
Magnesium (mEq/24 h)	0.22 ± 0.05	0.10 ± 0.01*	0.04	0.13*
Urine volume (ml/24 h)	11.1 ± 0.1	22.4 ± 2.4†	0.26‡	–

Values are mean ± SEM
*$P \le 0.05$, **$P \le 0.02$, †$P \le 0.005$, ‡$P \le 0.001$

embedded tissues. Firstly, crystal deposits were more common in the cortex than previously reported. Secondly, while most deposits were in the lumens of the collecting ducts, a few were in the lumens of the proximal tubules (Fig. 4a, b). These sections also revealed several deposits that were clearly not localized to the lumens (Fig. 4c, d). Whether these were located intracellularly or between cells could not be determined at the magnification used. Papillary crystals were somewhat more common in frozen sections; occasionally several

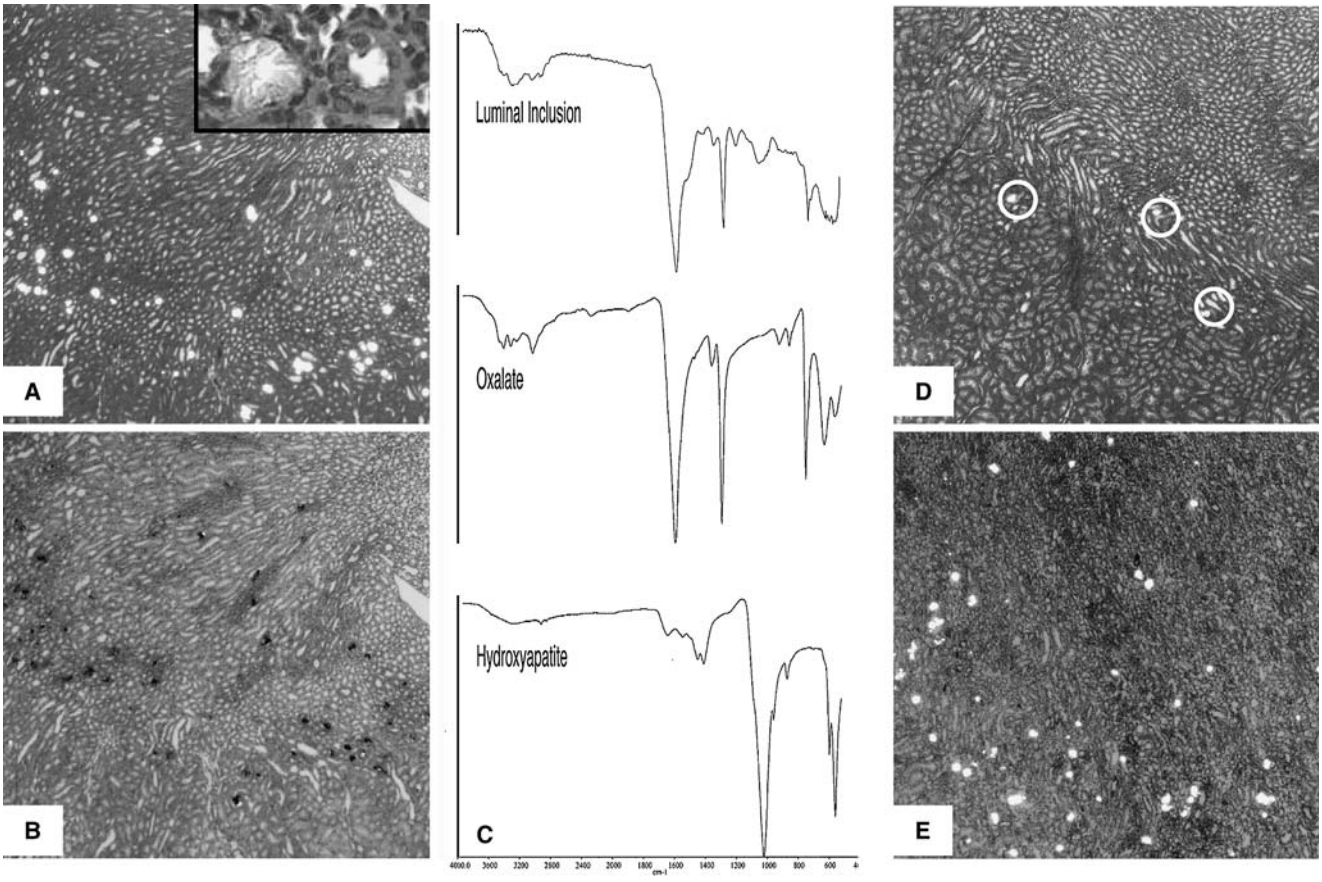

Fig. 3 Identification of the crystalline composition of deposits and comparison of tissue processing protocols. **a**, **b** Serial sections from a rat treated with 360 μmol/day KOx for 13D. Sections were embedded in paraffin, stained with H&E and photographed under polarizing optics (**a**) or the Yasue stain + H&E (**b**), 4× (*inset* 40×). **c** Representative tracing of μFTIR of Yasue positive staining deposit. **d**, **e** The effects of tissue processing on the number of observed crystals. Tissue from a rat treated with 360 μmol/day KOx for 13D was processed by standard immersion fixation in 4% paraformaldehyde, embedded in paraffin, and stained with H&E (**d**) or snap frozen, crysosectioned, fixed with 0.5 % glutaraldehyde and stained with Toluidine blue (**e**). Sections were photographed under polarizing optics at 4×. *Circles* birefringent deposits in the paraffin embedded section

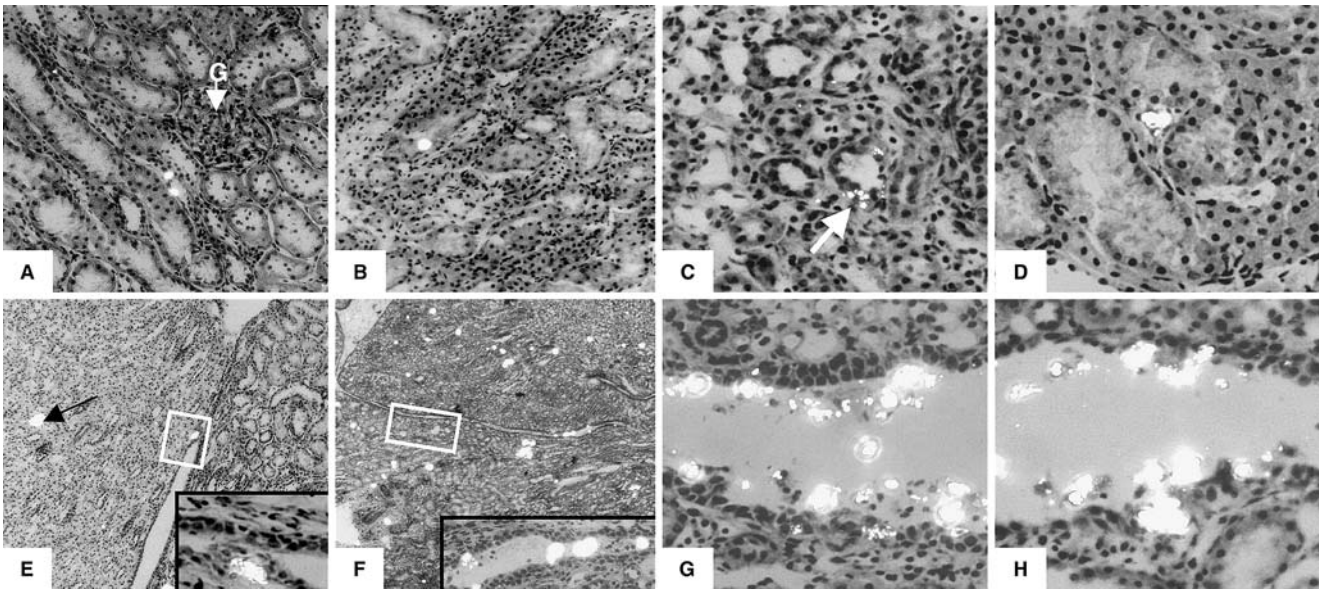

Fig. 4 Additional sites of calcium oxalate crystal deposition revealed using frozen sections, glutaraldehyde fixation, Toluidine blue staining and polarizing optics. **a** Deposition of crystals in the collecting ducts of the cortex, 20×. *G* glomerulus. **b** Deposition of crystals in the proximal tubules of the cortex, 20×. **c**, **d** Extraluminal deposition of crystals, 40×. **c** *White arrow* extraluminal deposit. **e** Deposition of crystals under the urothelium covering the papilla, 10×. **e** *Black arrow* papillary deposit. **e** *Inset* 40×. **f**, **g**, **h** Crystals deposited in the calyces. Note the very close apposition of the crystals to the papillary urothelium or cellular debris in (**g**, **h**). **f** 4×. **f** *Inset* 20×. **g**, **h** 40×

deposits were present, although one or two were more typical (Fig. 4e, arrow F). Interestingly, a few deposits were located just under the papillary urothelium (Fig. 4e, inset) or were present within the calyces and in close apposition to the papillary epithelium (Fig. 4f–h).

Discussion

This report describes an updated version of the minipump model characterized by continuous and steady delivery of oxalate for up to 2 weeks. This model will facilitate the study of oxalate's effects on the physiology of various organs including the kidney. The minipump model has an advantage over precursor models in that it cannot cause confounding effects due either to variable metabolism of a precursor to oxalate [34] or to production of extraneous and potentially nephrotoxic metabolites [35]. Hyperoxaluria develops within 0–12 h (data not shown) and crystalluria is readily detectable by D3 [24] and often earlier (data not shown).

Rats treated with 360 μmol/day KOx oxalate gained less weight than their PBS treated counterparts. However, there was no difference between the two groups for several other important parameters of rat health including blood chemistries, two tests of general renal function, levels of markers for systemic inflammatory response, and food consumption per gram of body weight. Analysis of urine chemistries revealed changes in the excretion of several ions, the meaning of which is not clear. Changes in the excretion of urinary ions have also been reported in other studies of continuous hyperoxaluria, but specifics differ between studies except as to decreased excretion of calcium [36–40]. It has been assumed that the hypocalciuria was due to the deposition of CaOx crystals throughout the body. While there is no direct data on this issue, infusions of oxalate labeled with ^{14}C have shown that it distributes widely throughout the body [41, 42, Marengo, unpublished observations], making this hypothesis plausible. As with the ethylene glycol and hydroxyproline oxalate precursor models of continuous hyperoxaluria [39, 43, 44], the minipump model is characterized by increased urine volume. Originally, this effect was considered to be an artifact attributable to excessive water consumption promoted by the sweet taste of ethylene glycol. However, this explanation is negated by the increased urine volume seen in rats treated with ethylene glycol by gavage, fed chow supplemented with hydroxyproline, or treated with oxalate subcutaneously by the minipump model. Using a continuous microperfusion system, Wareing and Green [45] showed that concentrations of luminal oxalate less than 0.05 mM stimulate fluid reabsorption while higher concentrations inhibit it. The excretion of several ions and water are tightly coupled; thus, changes in the reabsorption of a given ion or water could have a ripple effect on the reabsorption of other ions.

We were able to adjust the amount of hyperoxaluria and the incidence of CaOx crystalluria by adjusting the dosage of oxalate. All dosages of oxalate significantly increased oxalate excretion compared to that of PBS

rats. Treatment with 60 μmol/day KOx elevated urine oxalate excretion 2.8-fold over that of the PBS rats and induced sporadic crystalluria. Treatment with the next higher dose, 120 μmol/day KOx, increased oxalate excretion 3.8-fold over that of PBS rats and induced more consistent crystalluria. These dosages increase oxalate excretion to levels like those in Sprague–Dawley rats fed a diet supplemented with the oxalate precursor 5.2% hydroxyproline [46].

If one estimates the average oxalate excretion in humans to be ~30 mg of oxalate/day [6, 47], then many CaOx stone formers and individuals with mild enteric hyperoxaluria excrete ~1.5–4 times more oxalate than "normal" individuals [9, 48]. This degree of elevation is similar to that induced by 60 and 120 μmol/day KOx. However, the pattern of excretion differs despite this similarity. Minipump rats maintain a steady level of hyperoxaluria throughout the 13D treatment period, whereas it is hypothesized that many idiopathic CaOx stone formers experience only transient elevations in urinary oxalate due to variations in factors such as diet and hydration (and, of course, these elevations are repeated over months or years instead of 13D).

Treatment with higher doses of KOx increased oxalate excretion to levels like those in Sprague–Dawley rats drinking water supplemented with the oxalate precursor ethylene glycol [37, 43, 44, 49–51]. As expected, crystalluria was observed in most rats at most time points at the higher dosages of KOx. Patients with primary hyperoxaluria or severe enteric hyperoxaluria have continuous elevations in their oxalate excretion and can easily excrete 100–300 mg of oxalate/day [1, 8, 52, 53], which would place excretion at 3- to 10-fold of normal. This sustained high level is similar to that of rats treated with 240–360 μmol/day KOx.

CaOx-nephrocalcinosis was detectable by D13 in all rats treated with 360 μmol/day KOx. CaOx deposits were most common in the lumens of the collecting ducts near the corticomedullary junctions, although nonluminal deposits and nonmedullary deposits were also present. Of especial interest were the deposits just under and in close apposition to the papillary urothelium, since it has been speculated that crystals deposited in the interstitium of the outer papilla can erupt through the urothelium [32, 40, 54]. We had expected that the incidence of nephrocalcinosis would be somewhat proportional to the dosages of oxalate. Instead, both the incidence and the amount of crystal deposition in 300 μmol/day KOx rats were surprisingly less than in 360 μmol/day KOx rats, even though the dosage was only 17% lower. Both groups had similar growth characteristics, CRP levels and urine volumes, supporting the hypothesis that oxalate does not induce intrarenal crystal deposition by systemic effects. Both groups had consistent crystalluria during the postimplantation periods, suggesting that CaOx supersaturation was sufficient for crystallogenesis in both groups. It seems likely that intrarenal oxalate levels in the 360 μmol/day KOx rats exceeded a critical threshold above which crystals are retained in the tubules. Future studies will determine whether this threshold—assuming it exists—marks the induction of a high level of supersaturation (permitting very rapid crystal growth so that the crystals become trapped within the tubule lumens) and/or if it marks the induction of changes in the renal epithelium (allowing the crystals to adhere to the tubule walls). Because the intrarenal crystals are generally located in a fairly straight portion of the tubule, we favor the later explanation.

In its current configuration the minipump model most closely represents the type of enteric hyperoxaluria which develops in jejunoileal bypass patients [55–57], in that there is a sustained, 2-fold plus elevation in urinary oxalate excretion and deposition of birefringent CaOx crystals (i.e., CaOx-nephrocalcinosis) within the lumens of the collecting ducts. Interestingly, such patients can develop end stage renal failure due to CaOx-nephrocalcinosis without ever having developed a true CaOx stone [55, 57, 58]. Although CaOx-nephrocalcinosis is the general rule for bypass patients, there is a recent report involving four intestinal bypass patients with enteric hyperoxaluria in which the intraluminal deposits were not birefringent [9]. X-ray diffraction confirmed that these deposits were composed of hydroxyapatite, not CaOx. The reason for this discrepancy is not clear. The proportion of calcium phosphate in the stones increased with successive episodes [59, 60]. The four bypass patients had been stone free prior to bypass surgery and had at least two CaOx stones since then. In contrast, several patients in the earlier studies went into oxalate induced renal failure having passed one or no stones. A new rat model of intestinal resection found CaOx, apatite, and calcium carbonate crystals filling cortical proximal tubules and medullary collecting duct lumens with associated tubular obstruction and interstitial inflammation. These data suggest that the proportions of CaOx and apatite in renal crystals may transition through stages [40]. While deposition of any crystalline material in the kidney can be problematic, it could be argued that patients who can adjust their physiology to deposit hydryoxyapatite crystals rather than CaOx may be better off. Reports of patients losing kidneys due to massive deposits of hydroxyapatite are virtually nonexistent. One potentially valuable application of the minipump model would be to investigate what conditions are needed to cause deposition of hydroxyapatite in the presence of hyperoxaluria.

Conclusions

The development of an animal model for human disease always presents a number of challenges, especially when the disease results from the interaction of multiple genetic, physiologic and environmental factors. Often a variety of models is needed to gain a full appreciation of the pathology and the potential targets for treatment. The osmotic minipump makes possible an oxalate direct in vivo model for the study of CaOx nephrocalcinosis

and interactions between oxalate and the kidney. Dosages and length of treatment can be altered to provide different levels of hyperoxaluria, crystalluria and nephrocalcinosis, which will facilitate study of the milder forms of hyperoxaluria in humans.

Acknowledgements This manuscript is dedicated to the late Nicholas T. Stowe, without whose assistance this work could not have been completed. Appreciation is expressed to SE Brown for editorial assistance. This work was supported by NIH-NIDDK:DK55528 (SRM), DK62073 (SRM), NIH PO1 DK56788 (APE) and the Jim & Eilleen Dicke Research Endowment.

References

1. Milliner DS, Wilson DM, Smith LH (2001) Phenotypic expression of primary hyperoxaluria: comparative features of types I and II. Kidney Int 59:31
2. Bohles H, Beifuss OJ, Brandl U, Pichl J, Akcetin Z, Demling L (1988) Urinary factors of kidney stone formation in patients with Crohn's disease. Klin Wochenschr 66:87
3. Hocking MP, Duerson MC, O'Leary JP, Woodward ER (1983) Jejunoileal bypass for morbid obesity. Late follow-up in 100 cases. N Engl J Med 308:995
4. Annuk M, Backman U, Holmgren K, Vessby B (1998) Urinary calculi and jejunoileal bypass operation. A long-term follow-up. Scand J Urol Nephrol 32:177
5. Perez-Brayfield MR, Caplan D, Gatti JM, Smith EA, Kirsch AJ (2002) Metabolic risk factors for stone formation in patients with cystic fibrosis. J Urol 167:480
6. Curhan GC, Willett WC, Speizer FE, Stampfer MJ (2001) Twenty-four-hour urine chemistries and the risk of kidney stones among women and men. Kidney Int 59:2290
7. Asplin JR, Parks JH, Chen MS, Lieske JC, Toback FG, Pillay SN, Nakagawa Y, Coe FL (1999) Reduced crystallization inhibition by urine from men with nephrolithiasis. Kidney Int 56:1505
8. Menon M, Resnick MI (2002) Urinary lithiasis: etiology, diagnosis, and medical management. In: Walsh PC (ed) Campbell's urology, 8th edn. Saunders, Philadelphia, p 2229
9. Evan AP, Lingeman JE, Coe FL, Parks JH, Bledsoe SB, Shao Y, Sommer AJ, Paterson RF, Kuo RL, Grynpas M (2003) Randall's plaque of patients with nephrolithiasis begins in basement membranes of thin loops of Henle. J Clin Invest 111:607
10. Vermeulen CW, Lyon ES (1968) Mechanisms of genesis and growth of calculi. Am J Med 45:684
11. Khan SR, Finlayson B, Hackett RL (1983) Experimental induction of crystalluria in rats using mini-osmotic pumps. Urol Res 11:199
12. Khan SR, Finlayson B, Thomas WCJ, Hackett RL (1984) Relationship between experimentally induced crystalluria and relative supersaturation of various stone salts in rats. Urol Res 12:271
13. Holmes RP, Ambrosius WT, Assimos DG (2005) Dietary oxalate loads and renal oxalate handling. J Urol 174:943
14. Finlayson B, Reid F (1978) The expectation of free and fixed particles in urinary stone disease. Invest Urol 15:442
15. Thamilselvan S, Khan SR, Menon M (2003) Oxalate and calcium oxalate mediated free radical toxicity in renal epithelial cells: effect of antioxidants. Urol Res 31:3
16. Jonassen JA, Cao LC, Honeyman T, Scheid CR (2003) Mechanisms mediating oxalate-induced alterations in renal cell functions. Crit Rev Eukaryot Gene Expr 13:55
17. Chaturvedi LS, Kou lS, Sekhon A, Bhandari A, Menon M, Koul HK (2002) Oxalate selectively activates p38 mitogen-activated protein kinase and c-Jun N-terminal kinase signal transduction pathways in renal epithelial cells. J Biol Chem 277:13321
18. Khan SR, Thamilselvan S (2000) Nephrolithiasis: a consequence of renal epithelial cell exposure to oxalate and calcium oxalate crystals. Mol Urol 4:305
19. Scheid CR, Koul HK, Kennington L, Hill WA, Luber-Narod J, Jonassen J, Honeyman T, Menon M (1995) Oxalate-induced damage to renal tubular cells. Scanning Microsc 9:1097
20. Wiessner JH, Hasegawa AT, Hung LY, Mandel NS (1999) Oxalate-induced exposure of phosphatidylserine on the surface of renal epithelial cells in culture. J Am Soc Nephrol 10:S441
21. Verkoelen CF, van der Boom BG, Houtsmuller AB, Schroder FH, Romijn JC (1998) Increased calcium oxalate monohydrate crystal binding to injured renal tubular epithelial cells in culture. Am J Physiol 274:F958
22. Wiessner JH, Hasegawa AT, Hung LY, Mandel GS, Mandel NS (2001) Mechanisms of calcium oxalate crystal attachment to injured renal collecting duct cells. Kidney Int 59:637
23. Fasano JM, Khan SR (2001) Intratubular crystallization of calcium oxalate in the presence of membrane vesicles: an in vitro study. Kidney Int 59:169
24. Marengo SR, Chen DH-C, MacLennan GT, Resnick MI, Jacob GH (2004) Minipump induced hyperoxaluria and crystal deposition in rats: a model for calcium oxalate urolithiasis. J Urol 171:1304
25. Yasue T (1969) Histochemical identification of calcium oxalate. Acta Histochem Cytochem 2:83
26. Anderson JC, Dellomo JM, Sommer AJ, Evan AP, Bledsoe SB (2005) A concerted protocol for the analysis of mineral deposits in biopsied tissue using infrared microanalysis. Urol Res (in press)
27. Anderson J, Dellomo J, Sommer A, Evan A, Bledsoe S (2005) A concerted protocol for the analysis of mineral deposits in biopsied tissue using infrared microanalysis. Urol Res 33:213
28. Wilhelm SM, Stowe NT, Robinson AV, Schulak JA (2001) The use of the endothelin receptor antagonist, tezosentan, before or after renal ischemia protects renal function. Transplantation 71:211
29. Hirschfield GM, Pepys MB (2003) C-reactive protein and cardiovascular disease: new insights from an old molecule. Q J Med 96:793
30. Szalai AJ (2002) The biological functions of C-reactive protein. Vascul Pharmacol 39:105
31. Diaz Padilla N, Bleeker WK, Lubbers Y, Rigter GM, Van Mierlo GJ, Daha MR, Hack CE (2003) Rat C-reactive protein activates the autologous complement system. Immunology 109:564
32. de Beer FC, Baltz ML, Munn EA, Feinstein A, Taylor J, Bruton C, Clamp JR, Pepys MB (1982) Isolation and characterization of C-reactive protein and serum amyloid P component in the rat. Immunology 45:55
33. Evan AP, Bledsoe SB, Connors BA, Deng L, Liang L, Shao C, Fineberg NS, Grynpas MD, Stambrook PJ, Youzhi S, Sahota A, Tischfield JA (2001) Sequential analysis of kidney stone formation in the Aprt knockout mouse. Kidney Int 60:910
34. Fan J, Chandhoke PS, Grampsas SA (1999) Role of sex hormones in experimental calcium oxalate nephrolithiasis. J Am Soc Nephrol 10:S376
35. Poldelski V, Johnson A, Wright S, Rosa VD, Zager RA (2001) Ethylene-glycol-mediated tubular injury:identification of critical metabolites and injury pathways. Am J Kidney Dis 38:339
36. Khan SR (1995) Animal model of calcium oxalate nephrolithiasis. In: Khan SR (ed) Calcium oxalate in biological systems. CRC Press Inc., New York, p 343
37. Fan J, Glass MA, Chandhoke PS (1998) Effect of castration and finasteride on urinary oxalate excretion in male rats. Urol Res 26:71
38. Asselman M, Verhulst A, De Broe ME, Verkoelen CF (2003) Calcium oxalate crystal adherence to hyaluronan-, osteopontin-, and CD44-expressing injured/regenerating tubular epithelial cells in rat kidneys. J Am Soc Nephrol 14:3155
39. Bushinsky DA, Asplin JR, Grynpas MD, Evan AP, Parker WR, Alexander KM, Coe FL (2002) Calcium oxalate stone formation in genetic hypercalciuric stone-forming rats. Kidney Int 61:975

40. O'Connor RC, Worcester EM, Evan AP, Meehan S, Kuznetsov D, Laven B, Sommer AJ, Bledsoe SB, Parks JH, Coe FL, Grynpas M, Gerber GS (2005) Nephrolithiasis and nephrocalcinosis in rats with small bowel resection. Urol Res 33:105
41. Costello JF, Smith M, Stolarski C, Sadovnic MJ (1992) Extrarenal clearance of oxalate increases with progression of renal failure in the rat. J Am Soc Nephrol 3:1098
42. Sugimoto T, Osswald H, Yamamoto K, Kanazawa T, Iimori H, Funae Y, Kamikawa S, Kishimoto T (1993) Fate of circulating oxalate in rats. Eur Urol 23:485
43. Green ML, Hatch M, Freel RW (2005) Ethylene Glycol Induces Hyperoxaluria without metabolic acidosis in rats. Am J Physiol Renal Physiol 289:F536
44. Thamilselvan S, Menon M (2005) Vitamin E therapy prevents hyperoxaluria-induced calcium oxalate crystal deposition in the kidney by improving renal tissue antioxidant status. BJU Int 96:117
45. Wareing M, Green R (1994) Effect of formate and oxalate on fluid reabsorption from the proximal convoluted tubule of the anaesthetized rat. J Physiol 477:347
46. Khan SR, Shevock PN, Hackett RL (1989) Urinary enzymes and calcium oxalate urolithiasis. J Urol 142:846
47. Pirulli D, Marangella M, Amoroso A (2003) Primary hyperoxaluria: genotype-phenotype correlation. J Nephrol 16:297
48. Parks JH, Worcester EM, O'Connor RC, Coe FL (2003) Urine stone risk factors in nephrolithiasis patients with and without bowel disease. Kidney Int 63:255
49. de Water R, Boeve ER, van Miert PPMC, Deng G, Cao LC, Stijnen T, de Bruijn WC, Schroder FH (1996) Experimental nephrolithiasis in rats: the effect of ethylene glycol and vitamin D3 on the induction of renal calcium oxalate crystals. Scanning Microsc 10:591
50. Umekawa T, Hatanaka Y, Kurita T, Khan SR (2004) Effect of angiotensin II receptor blockage on osteopontin expression and calcium oxalate crystal deposition in rat kidneys. J Am Soc Nephrol 15:635
51. Toblli JE, Ferder L, Stella I, De Cavanaugh EM, Angerosa M, Inserra F (2002) Effects of angiotensin II subtype 1 receptor blockade by losartan on tubulointerstitial lesions caused by hyperoxaluria. J Urol 168:1550
52. Coe FL, Parks JH, Asplin JR (1992) The pathogenesis and treatment of kidney stones. NEJM 327:1141
53. Monico CG, Persson M, Ford GC, Rumsby G, Milliner DS (2002) Potential mechanisms of marked hyperoxaluria not due to primary hyperoxaluria I or II. Kidney Int 62:392
54. Khan SR (1995) Mechanisms involved in calcium oxalate nephrolithiasis based on studies in an animal model. Ital J Miner Electrolyte Metab 9:3
55. Mole DR, Tomson CR, Mortensen N, Winearls CG (2001) Renal complications of jejuno-ileal bypass for obesity. QJM 94:69
56. Hassan I, Juncos LA, Milliner DS, Sarmiento JM, Sarr MG (2001) Chronic renal failure secondary to oxalate nephropathy: a preventable complication after jejunoileal bypass. Mayo Clin Proc 76:758
57. Drenick EJ, Stanley TM, Border WA, Zawada ET, Dornfeld LP, Upham T, Llach F (1978) Renal damage with intestinal bypass. Ann Intern Med 89:594599
58. Hicks K, Evans GB, Rogerson ME, Bass P (1998) Jejuno-ileal bypass, enteric hyperoxaluria, and oxalate nephrosis: a role for polarised light in the renal biopsy. J Clin Pathol 51:700
59. Mandel N, Mandel I, Fryjoff K, Rejniak T, Mandel G (2003) Conversion of calcium oxalate to calcium phosphate with recurrent stone episodes. J Urol 169:2026
60. Parks JH, Worcester EM, Coe FL, Evan AP, Lingeman JE (2004) Clinical implications of abundant calcium phosphate in routinely analyzed kidney stones. Kidney Int 66:777